Escape of O^+ through the distant tail plasma sheet

L. M. Kistler,[1] A. B. Galvin,[1] M. A. Popecki,[1] K. D. C. Simunac,[1] C. Farrugia,[1] E. Moebius,[1] M. A. Lee,[1] L. M. Blush,[2] P. Bochsler,[2] P. Wurz,[2] B. Klecker,[3] R. F. Wimmer-Schweingruber,[4] A. Opitz,[5] J.-A. Sauvaud,[5] B. Thompson,[6] and C. T. Russell[7]

Received 11 August 2010; revised 13 September 2010; accepted 17 September 2010; published 3 November 2010.

[1] In February 2007, the STEREO-B spacecraft encountered the magnetosheath, plasma sheet and plasma sheet boundary layer from about 200 R_E to 300 R_E downtail. This time period was during solar minimum, and there was no storm activity during this month. Using data from the PLASTIC instrument, we find that even during quiet times, O^+ is a constant feature of the deep magnetotail, with an O^+ density of about 15% of the O^+ density in the near-earth plasma sheet for similar conditions. The tailward flux of the O^+ is similar to the flux of O^+ beams that have been observed in the lobe/mantle region of the deep tail. The total outflow rate of the O^+ down the plasma sheet is 1.1×10^{24} ions/s, which is 10% of the total outflow rate of 1×10^{25} ions/s, and of the same order as the estimated loss from dayside transport. **Citation:** Kistler, L. M., et al. (2010), Escape of O^+ through the distant tail plasma sheet, *Geophys. Res. Lett.*, *37*, L21101, doi:10.1029/2010GL045075.

1. Introduction

[2] During quiet solar and geomagnetic times, the total outflow from the ionosphere is on the order of 1×10^{25} ions/s [*Yau and Andre*, 1997]. However, the fraction of this O^+ that eventually escapes completely from the magnetosphere is not known. *Seki et al.* [2001] identified four pathways for ion escape, and estimated the amount of loss through each pathway. The four pathways are the escape of plasmaspheric ions out the front side magnetosphere, the drift of ions from the plasma sheet and ring current to the front side magnetosphere, the escape of cusp-origin ions tailward through the lobe/mantle region, and the escape of ions tailward through the plasmasheet, either through plasmoids or through the non-plasmoid plasma sheet, tailward of the distant neutral line. While there have been previous measurements of O^+ in the distant tail [e.g., *Christon et al.*, 1994; *Lui et al.*, 1994; *Zong et al.*, 1997], there have been no estimates of the amount of O^+ escaping through this final path, either through plasmoids or through the quiescent plasma sheet, because the previous measurements have predominantly been of energetic particles.

[3] O^+ has also been observed in the deep tail in the lobe/mantle region [e.g., *Seki et al.*, 1998]. These observations show that cold O^+ beams, which likely originate in the cusp/cleft region, are observed as far down the tail as 200 R_E. Their observed velocity increases with downtail distance, and they co-exist with field aligned proton distributions of solar wind origin that are at nearly the same velocity.

[4] In this paper we report observations by the PLASTIC instrument on STEREO-B of tailward flowing O^+ observed in the deep tail. STEREO-B was in the magnetosheath and magnetotail in February 2007, a period during solar minimum. There were no geomagnetic storms reported that month. Thus the measurements here represent a time of low ionospheric input, providing a baseline for the amount of O^+ present in the distant tail.

2. Instrumentation

[5] Measurements in this paper are from the PLASTIC instrument [*Galvin et al.*, 2008] and the magnetometer [*Acuna et al.*, 2008] on the STEREO spacecraft. The PLASTIC instrument is designed to measure the solar wind and suprathermal ion composition over the energy range 200 eV/e to 80 keV/e. The PLASTIC instrument is divided into a "solar wind sector" that covers 45° in the sunward direction in the ecliptic plane, and +/− 20° out of the ecliptic plane and the "wide angle partition" that covers the rest of the ecliptic plane, with some gaps due to blockage, with an angular field of view of 3° out of the ecliptic. Thus, the instrument measures a good fraction of the 3D velocity distribution close to the ecliptic plane. Because the instrument's primary goal is to measure the solar wind, many of the data products used, including the routinely calculated moments, which are shown in Figures 1 and 2, only include data from the solar wind sector.

3. Observations

[6] Figure 1 shows the STEREO data from 6 February 2007 through 2 March 2007. During this time, STEREO B was located on the dusk side of the tail, north of the nominal neutral sheet, and moved from $(X,Y,Z)_{GSM}$ = (−143, 13.8, 57.6) to (−325, 68.2, 35.8) R_E. Figures 1a and 1b show the H^+ density and velocity measured by STEREO A (red) and B (black) in the solar wind sector. STEREO A was located upstream in the solar wind. Starting around 14 February 2007, the density measured by STEREO B drops signifi-

[1]Space Science Center, University of New Hampshire, Durham, New Hampshire, USA.
[2]Physikalisches Institut, University of Bern, Bern, Switzerland.
[3]Max-Planck Institute für Extraterrestriche Physik, Garching, Germany.
[4]Institute for Experimental and Applied Physics, University of Kiel, Kiel, Germany.
[5]CESR, Toulouse, France.
[6]NASA Goddard Space Flight Center, Greenbelt, Maryland, USA.
[7]Institute of Geophysics and Planetary Physics, University of California, Los Angeles, California, USA.

0094-8276/10/2010GL045075

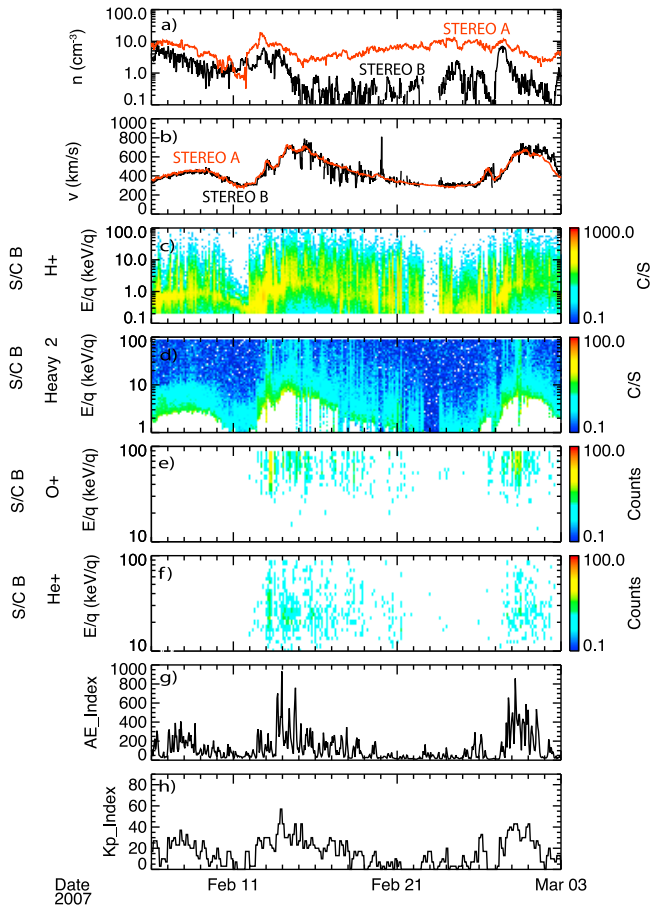

Figure 1. (a–h) STEREO/PLASTIC data and geomagnetic indices from 6 February to 2 March 2007.

cantly, compared to the solar wind. The velocities on the two spacecraft track through this time period, although the low count rate on STEREO B during the low density periods leads to more fluctuation in the velocity measurement. Figure 1c shows the proton energy spectra from STEREO B. The peak in the energy closely follows the changes in the solar wind velocity, as expected. However the spectrum is broad and extends to high energies, indicating that the spacecraft is in the magnetosheath or plasma sheet throughout this time period. Figure 1d shows energy spectra for the "Heavy 2" rate, which includes mainly low charge state heavy ions. Analysis of event data (not shown) indicates that above 20 keV, this rate is dominated by O^+ and He^+. Starting around 13 February, this rate shows bursts of energetic ions. O^+ is a clear indicator of an ionospheric source. He^+ may have an ionospheric origin, but is also present in the solar wind as an interstellar pick-up ion [*Moebius et al.*, 1985]. Figures 1e and 1f show the number of counts of O^+ and He^+, separately. The energetic bursts are dominated by O^+, whereas He^+ counts are found predominantly at lower energies. Figures 1g and 1h show the AE and Kp indices for this time period. The high-speed solar wind streams tend to correlate with higher geomagnetic activity, but the Kp remains low to moderate throughout this time period, and no storms were reported during this month.

[7] In this paper, we concentrate on an example of an O^+ observation, on 13 February 2007 when the spacecraft was located at $(X,Y,Z)_{GSM} \approx (-198, 20,45)$ R_E. Figure 2 shows a time period from 4:00–10:00 on this day. Figures 2a–2g show the proton velocity, density, and temperature, calculated in the solar wind sector, magnetic field components in GSM, and the total magnetic field. Values from STEREO B (A) are in black(red). Figures 2h–2j show the proton spectra over two energy ranges, 4–100 keV and 0.1–4 keV, and the angular distribution out of the ecliptic for the low energy H^+. Figure 2k shows the energetic O^+. The three clear time periods with energetic O^+ are enclosed by blue boxes. Each of the O^+ time periods is characterized by a decrease in density (Figure 2b) and an increase in temperature (Figure 2c). In addition, all three time periods show clear changes in the magnetic field. During the first time period, B_x changes from slightly negative to strongly positive, and B_y dips briefly from positive, as in the solar wind, towards zero. The second time period shows similar variations in the magnetic field, with B_x turning positive, and B_y moving towards zero. In the final period, B_x turns negative, while B_y again dips toward zero. When the spacecraft is in the magnetosheath, for example from 9:00–10:00, there are very few energetic particles, and the angular distribution of the low energy protons (Figure 2j) is highly peaked at 0°. During the O^+ time periods, energetic H^+ is observed, and the angular distribution of the low energy H^+ within the 40° range is isotropic. The magnetic field signatures, the changes in the moments, the energetic ions, and the broader angular distributions all indicate that the spacecraft has moved across the magnetopause into the northern plasma sheet or plasma-sheet boundary layer. That the spacecraft does not first encounter the lobe is most likely because it is located far on the dusk side.

[8] A spacecraft at 200 R_E is normally tailward of the distant neutral line [*Zwickl et al.*, 1984]. The observations presented here show that O^+ is escaping down the tail even in these solar and geomagnetically quiet time periods. To calculate the amount of O^+ observed, we concentrate on one time period, from 6:40 to 7:40. This time period was chosen because it is the longest excursion into the plasma sheet/boundary layer during this day, and so it allows us to accumulate sufficient statistics to obtain an O^+ spectrum. So far, we have shown data from the solar wind sector. We need to estimate the amount of plasma in the full 3D distribution in order to calculate the amount of O^+. Because the spacecraft is not in the solar wind or magnetosheath, the assumption that the full distribution is measured in the solar wind sector is likely no longer valid. However, previous observations have shown that on average, the plasma sheet plasma beyond 200 R_E is flowing downtail at a velocity similar to the solar wind speed [*Zwickl et al.*, 1984]. In addition, it has been shown that the suprathermal particle distribution can be consistent with an isotropic population convected down the tail [*Gloeckler et al.*, 1984; *Christon et al.*, 1994]. To test if that is the case, we compare the distributions flowing in the anti-sunward direction (the solar wind sector) with the distributions flowing in the sunward direction. Figure 3a shows H^+ and O^+ distribution functions averaged over this time period. For H^+, the distribution function is shown for the solar wind sector, and for the 8 angular positions on the opposite side of the instrument. This measurement uses a single-coincidence counting rate with high efficiency. The inset shows the locations of the positions, relative to the solar wind sector. Clearly the highest fluxes are observed flowing tailward (SW sector)

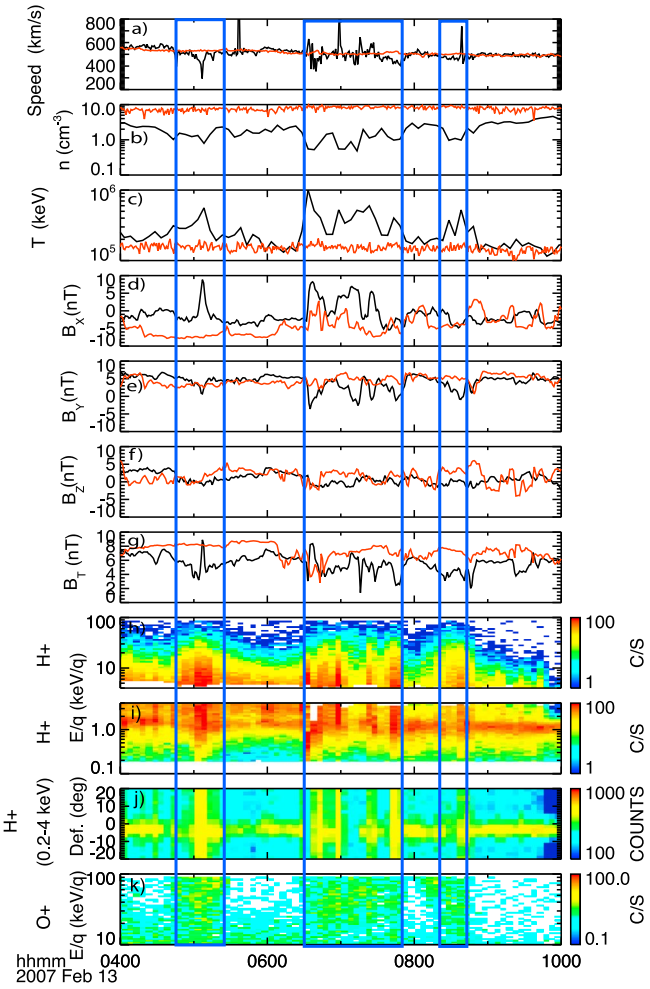

Figure 2. (a–k) STEREO A (red) and B (black) data for the time period 4:00–10:00, 13 February 2007.

and the lowest are observed flowing sunward (positions 1 and 2). Following *Gloeckler et al.* [1984], we assume that there is a frame in which the distribution is isotropic. Figure 3b shows the same spectra, but now in a frame moving tailward at 500 km/s. In this frame, the distributions from the different positions line up, validating the assumption. While agreement is not perfect, the positions agree within the uncertainties of the calibration for these positions.

[9] Low instrument efficiencies for composition data in the sunward flowing positions prevent us from performing the exact same test using the O^+ data. However, position 6, has good efficiency and sufficient counts to perform a similar test. Figure 3a also shows the O^+ distribution functions from the solar wind sector and from position 6. Again, making the assumption that the population is isotropic, and moving tailward at 500 km/s, this position will only have a small velocity shift, because it is almost perpendicular to the direction of motion. As shown in Figure 3b, when shifted using the same assumptions, these distributions also line up well.

[10] By integrating over the measured energy range, and assuming isotropy in the plasma rest frame, we determine the density of the bulk O^+ and H^+ populations flowing down the tail. The results of the density calculations are given in Table 1. The H^+ density is 4.31 cm^{-3}, while the O^+ density is 2.79×10^{-4} cm^{-3}. The net flux of O^+ down the tail, calculated by multiplying the density by the velocity, 500 km/s is 1.4×10^4 cm^{-2} s^{-1}.

[11] To compare these measurements with measurements in the near-earth plasma sheet under similar conditions we use the Cluster/CODIF instrument [*Rème et al.*, 1997]. In October–November 2006, the Cluster apogee was in the dusk-side plasma sheet. We have scanned the Cluster data for October and November 2006 to find time periods when Cluster is in the plasma sheet, the Dst index is low, so that there is no storm activity, and the solar wind speed is similar to that during our STEREO event, around 500 km/s. Five time periods met these criteria. The specific times, the Dst, Kp, F10.7, and solar wind velocities during these intervals are given in Table 1. Figure 4a shows the comparisons of the O^+ phase space density at STEREO and in the near-earth plasma sheet. The spectra from both spacecraft are shown in the plasma rest frame, which is a frame with no bulk velocity for Cluster, and is a frame moving at 500 km/s for STEREO. The O^+ phase space density at Cluster is about a factor of 10 higher than at STEREO. The comparison of the proton distributions is shown in Figure 4b. At high velocities, the distribution function is again about a factor of 10 higher at Cluster than at STEREO. However at lower velocities, the protons exceed the value at Cluster, and have a magnetosheath-like spectrum. STEREO is very close to the magnetosheath, and is most likely in a boundary layer region. Table 1 lists the densities for each of the time periods, and gives an average for the five Cluster time periods. The O^+ density at STEREO, at 200 R_E, is about 15% of the O^+ density at Cluster, in the near-earth tail. The STEREO H^+ density is higher than the Cluster density, most likely

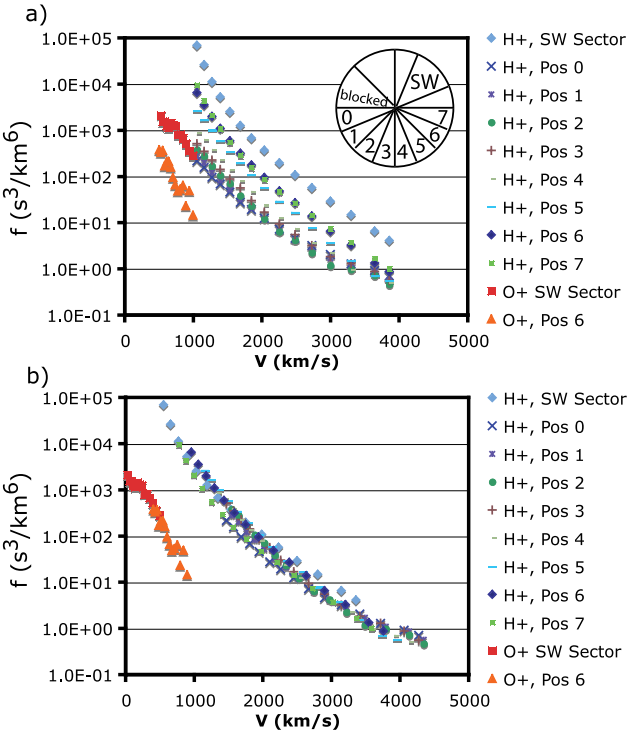

Figure 3. (a) H^+ and O^+ distribution functions in the spacecraft frame. (b) The same spectra now assuming a frame moving tailward at 500 km/s.

Table 1. H^+ and O^+ Densities for STEREO in the Deep Tail and Cluster in the Near-Earth Tail, and the Associated Dst, Kp, F10.7 and Solar Wind Velocity During These Times

	H+ (1/cm^3)	O+ (1/cm^3)	Dst	Kp	Vsw (km/s)	F10.7
STEREO 2007/02/13 6:40-7:40	4.31E+00	2.79E-04	−7	2+	490	70.9
Cluster Average	1.11E-01	1.80E-03	−11.6	1+	491.2	78.9
2006/Oct/02 8:30-11:30.	1.24E-01	2.83E-03	−13	1+	480	78
2006/Oct/23 18:00-22:00.	1.90E-01	1.80E-03	−5	1+	515	75.7
2006/Oct/30 20:00-24:00.	1.13E-01	1.05E-03	−15	1	497	74.6
2006/Nov/28 16:10-17:40.	8.20E-02	2.21E-03	−16	2−	483	83.2
2006/Nov/28 10:00-12:30.	4.70E-02	1.09E-03	−9	1+	481	83.2

because of the larger solar wind ion contribution in the boundary layer.

[12] If we assume that the O^+ flux we observe is constant across the plasma sheet, we can estimate the total O^+ lost down the plasma sheet during quiet times. While our observations are made in a boundary layer region, the O^+ spectrum and the high energy portion of the H^+ spectrum appear typical for plasma sheet, making this assumption reasonable. By assuming that the plasma sheet is 40 R_E wide [*Seki et al*, 2001] and 5 R_E thick [*Pulkkinen et al.*, 1993; *Christon et al.*, 1998] we end up with a total outflow of 1.1 × 10^{24} ions/s lost through this pathway.

4. Discussion

[13] The time period discussed in this paper is during solar minimum, and there was no geomagnetic storm activity. In addition, we do not observe signatures of plasmoids in the magnetic field. Plasmoids are normally associated with a bipolar signature in B_z, and sometime B_y, and an increase in total pressure [*Ieda et al.*, 1998], and neither of these are observed in our case. Thus our interpretation is that during this time we are observing the quiet plasma sheet boundary layer on the dusk flank, adjacent to the magnetosheath, and tailward of the neutral line.

[14] For O^+ to escape through the quiescent plasma sheet tailward of the distant neutral line, it must first be transported to the distant tail. When field lines reconnect at the distant neutral line, the field lines, and the plasma on these field lines move from the lobe mantle region into the plasma sheet. Thus the O^+ that we observed is likely entering from the lobe. *Seki et al.* [2001] calculate the flux for the O^+ beams that have been observed in the deep tail lobe. They find that the flux of the beams predominantly falls in the range from 5 × 10^3 $cm^{-2}s^{-1}$ to 5 × 10^4 $cm^{-2}s^{-1}$. Thus the flux observed in the plasma sheet at this time, 1.1 × 10^4 cm^{-2} s^{-1}, falls right in the range of the flux of the beams observed in the tail. *Seki et al.* [1998] also showed a strong Kp dependence in the occurrence frequency of the beams, with only 10% of the observations containing O^+ for Kp = 2. Thus, while our flux values are consistent with the beams in general, it is still surprising that we see significant O^+ during this time. We speculate that this may be due to a solar wind velocity dependence that enhances the O+ in the deep tail, even for low Kp. *Seki et al.* [1998] showed that the time periods with significant cold O^+ beams were the time periods when the mantle population had the highest velocity. Since this mantle population has its source in the solar wind, these times with high O^+ are likely to be times with high solar wind velocity. Thus, although the activity is low, the high solar wind velocity may be the factor that increases the transport of O^+ down the tail, from where it can then enter the distant plasma sheet.

[15] The rate of O^+ lost, 1.1 × 10^{24} ions/s, is ~10% of the total outflow from the ionosphere. *Seki et al.* [2001] estimated that the escape rate of the lobe/mantle beams is 1.6 × 10^{24} ions/s in the mid-tail (75–150 R_E) region, and 0.59 × 10^{24} ions/s in the far-tail (150–210 R_E) region. This gives a consistent picture that the beams continue to enter the plasma sheet through reconnection at the distant neutral line,

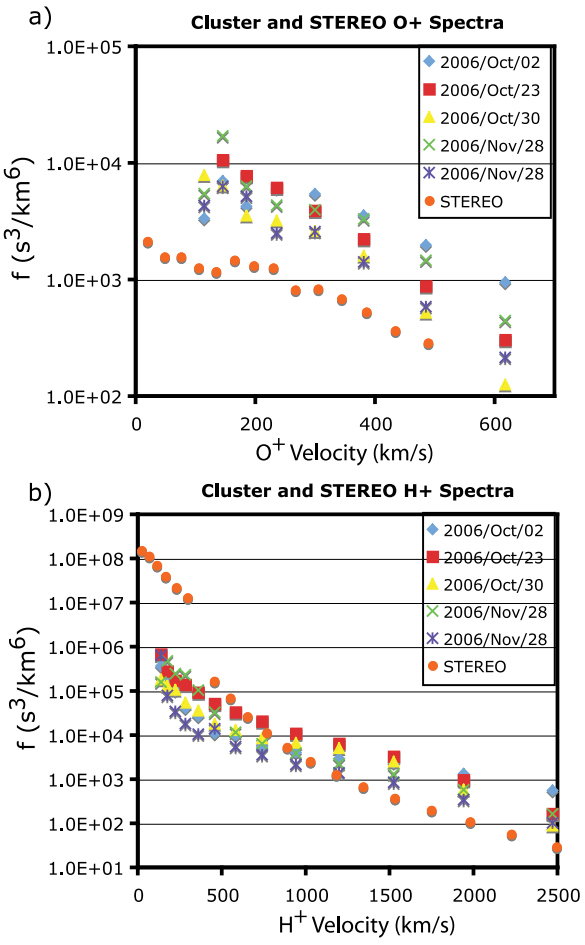

Figure 4. (a) O^+ STEREO/PLASTIC and Cluster/CODIF distribution functions, both in the rest frame, and (b) H^+ STEREO/PLASTIC and Cluster/CODIF distribution functions, both in the rest frame.

providing the source for the plasma sheet population. The loss rate is of the same order as the estimated loss through the front-side magnetopause pathways.

[16] **Acknowledgments.** Work at UNH was supported by NASA under contract NAS5-00132.

References

Acuna, M. H., D. Curtis, J. L. Scheifeie, C. T. Russell, P. Schroeder, A. Szabo, and J. G. Luhmann (2008), The STEREO/IMPACT magnetic field experiment, *Space Sci. Rev.*, doi:10.1007/s11214-007-9259-2.

Christon, S. P., et al. (1994), Energetic atomic and molecular ions of ionospheric origin observed in distant magnetotail flow-reversal events, *Geophys. Res. Lett.*, *21*, 3023–3026, doi:10.1029/94GL02095.

Christon, S. P., et al. (1998), Magnetospheric plasma regimes identified using Geotail measurements: 2. Statistics, spatial distribution, and geomagnetic dependence, *J. Geophys. Res.*, *103*, 23,521–23,542, doi:10.1029/98JA01914.

Galvin, A. B., et al. (2008), The Plasma and Suprathermal Ion Composition (PLASTIC) investigation on the STEREO observatories, *Space Sci. Rev.*, *136*, 437–486, doi:10.1007/s11214-007-9296-x.

Gloeckler, G., M. Scholer, F. M. Ipavich, D. Hovestadt, B. Klecker, and A. B. Galvin (1984), Abundances and spectra of suprathermal H+, He++ and heavy ions in a fast moving plasma structure (plasmoid) in the distant geotail, *Geophys. Res. Lett.*, *11*, 603–606, doi:10.1029/GL011i006p00603.

Ieda, A., S. Machida, T. Mukai, Y. Saito, T. Yamamoto, A. Nishida, T. Terasawa, and S. Kokubun (1998), Statistical analysis of the plasmoid evolution with Geotail observations, *J. Geophys. Res.*, *103*, 4453–4465, doi:10.1029/97JA03240.

Lui, A. T. Y., D. J. Williams, S. P. Christon, R. W. McEntire, V. Angelopoulos, C. Jacquey, T. Yamamoto, and S. Kokubun (1994), A preliminary assessment of energetic ion species in flux ropes/plasmoids in the distant tail, *Geophys. Res. Lett.*, *21*, 3019–3022, doi:10.1029/94GL01283.

Moebius, E., D. Hovestadt, B. Klecker, M. Scholer, and G. Gloeckler (1985), Direct observation of He^+ pick-up ions of interstellar origin in the solar wind, *Nature*, *318*, 426–429, doi:10.1038/318426a0.

Pulkkinen, T. I., D. N. Baker, C. J. Owen, J. T. Gosling, and N. Murphy (1993), Thin current sheets in the deep geomagnetic tail, *Geophys. Res. Lett.*, *20*, 2427–2430, doi:10.1029/93GL01590.

Rème, H., et al. (1997), The Cluster ion spectrometry experiment, *Space Sci. Rev.*, *79*, 303–350, doi:10.1023/A:1004929816409.

Seki, K., M. Hirahara, T. Terasawa, T. Mukai, Y. Saito, S. Machida, T. Yamamoto, and S. Kokubun (1998), Statistical properties and possible supply mechanisms of tailward cold O^+ beams in the lobe/mantle regions, *J. Geophys. Res.*, *103*, 4477–4489, doi:10.1029/97JA02137.

Seki, K., R. C. Elphic, M. Hirahara, T. Terasawa, and T. Mukai (2001), On atmospheric loss of oxygen ions from Earth through magnetospheric processes, *Science*, *291*, 1939–1941, doi:10.1126/science.1058913.

Yau, A. W., and M. Andre (1997), Sources of ion outflow in the high latitude ionosphere, *Space Sci. Rev.*, *80*, 1–25, doi:10.1023/A:1004947203046.

Zong, Q.-G., et al. (1997), Geotail observations of energetic ion species and magnetic field in plasmoid-like structures in the course of an isolated substorm event, *J. Geophys. Res.*, *102*, 11,409–11,428, doi:10.1029/97JA00076.

Zwickl, R. D., D. N. Baker, S. J. Bame, W. C. Feldman, J. T. Gosling, E. W. Hones Jr., D. J. McComas, B. T. Tsurutani, and J. A. Slavin (1984), Evolution of the Earth's distant magnetotail: ISEE 3 electron plasma results, *J. Geophys. Res.*, *89*, 11,007–11,012, doi:10.1029/JA089iA12p11007.

L. M. Blush, P. Bochsler, and P. Wurz, Physikalisches Institut, University of Bern, Sidelstrasse 5, CH-3012 Bern, Switzerland.

C. Farrugia, A. B. Galvin, L. M. Kistler, M. A. Lee, E. Moebius, M. A. Popecki, and K. D. C. Simunac, Space Science Center, University of New Hampshire, Morse Hall, Durham, NH 03824, USA. (lynn.kistler@unh.edu)

B. Klecker, Max-Planck Institute für Extraterrestriche Physik, Giessenbachstrasse, D-85748 Garching, Germany.

C. T. Russell, Institute of Geophysics and Planetary Physics, University of California, 3845 Slichter Hall, 603 Charles Young Drive E., Los Angeles, CA 90095-1567, USA.

A. Opitz and J.-A. Sauvaud, CESR, avenue du Colonel Roche, BP 4346, F- 31028 Toulouse CEDEX, France.

B. Thompson, NASA Goddard Space Flight Center, Code 682.3, Greenbelt, MD 20771, USA.

R. F. Wimmer-Schweingruber, Institute for Experimental and Applied Physics, University of Kiel, D-24098 Kiel, Germany.